Local Refractive Index Sensing Based on Edge Gold-Coated Silver Nanoprisms

ARTICLE *in* THE JOURNAL OF PHYSICAL CHEMISTRY C · OCTOBER 2013

Impact Factor: 4.77 · DOI: 10.1021/jp408187e

THE JOURNAL OF PHYSICAL CHEMISTRY C

Article

pubs.acs.org/JPCC

Local Refractive Index Sensing Based on Edge Gold-Coated Silver Nanoprisms

Erik Martinsson,[†] Mohammad Mehdi Shahjamali,[‡] Karin Enander,[†] Freddy Boey,[‡] Can Xue,[‡] Daniel Aili,*[,†] and Bo Liedberg[†,§]

[†]Division of Molecular Physics, Department of Physics, Chemistry and Biology (IFM), Linköping University, SE-581 83 Linköping, Sweden

[‡]School of Materials Science and Engineering, Nanyang Technological University, Block N4.1, 50 Nanyang Avenue, Singapore 639798

[§]Centre for Biomimetic Sensor Science, Nanyang Technological University, 50 Nanyang Drive, Research Technoplaza, Sixth Storey, XFrontiers Block, Singapore 637553

Supporting Information

ABSTRACT: Bulk and surface refractive index sensitivity for localized surface plasmon resonance (LSPR) sensing based on edge gold-coated silver nanoprisms (GSNPs) and gold nanospheres was investigated and compared with conventional surface plasmon resonance (SPR) sensing based on propagating surface plasmons. The hybrid GSNPs benefit from an improved stability since the gold frame protecting the unstable silver facets located at the silver nanoprisms (SNPs) edges and tips prevents truncation or rounding of their sharp tips or edges, maintaining a high refractive index sensitivity even under harsh conditions. By using layer-by-layer deposition of polyelectrolytes and protein adsorption, we found that GSNPs exhibit 4-fold higher local refractive index sensitivity in close proximity (<10 nm) to the surface compared to a flat gold film in the conventional SPR setup. Moreover, the sensitivity was 8-fold higher with GSNPs than with gold nanospheres. This shows that relatively simple plasmonic nanostructures for LSPR-based sensing can be engineered to outperform conventional SPR, which is particularly interesting in the context of detecting low molecular weight compounds where a small sensing volume, reducing bulk signals, is desired.

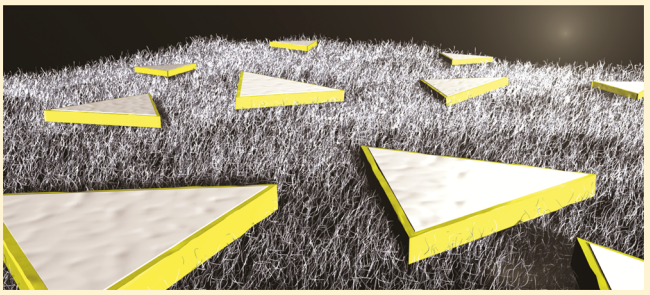

Surface plasmon resonance (SPR) is one of the most widely used optical techniques for label-free, real-time biosensing.[1] Conventional SPR analysis is based on propagating surface plasmons which are electromagnetic charge oscillations, excited at the interface between a thin metal film and a dielectric.[2] Excitation of surface plasmons using light results in a pronounced minimum in the reflectivity spectrum, where the condition for excitation is highly dependent on the refractive index (RI) in close proximity of the metal surface. This allows for sensitive detection of molecular events occurring at the metal interface, either using angular or spectral interrogation.[3] Today, conventional SPR is routinely used in several different areas and has evolved into a mature biosensing technology.[4−6]

Over the past decade, so-called localized surface plasmon resonance (LSPR) has received considerable interest.[7−9] LSPR is caused by collective electron oscillations confined in metal nanostructures and can typically be excited by visible or near-infrared light, where the resonance frequency is highly dependent on the shape, size, material, composition, surface modification, and aggregate morphology.[10−16] The resonance condition is also dependent on the polarizability of the surrounding medium. The possibility to use metal nanostructures for detection of small local refractive index changes and the possibility for integration and miniaturization has made LSPR-based sensing an attractive alternative to conventional SPR.[17]

Both sensing strategies utilize the plasmonic properties of noble metals and the strong electromagnetic field created at the plasmon resonance frequency. The intensity and decay length of the electromagnetic field are considerably different for propagating surface plasmons compared to localized surface plasmons which results in differences in both sensitivity (η) and sensing volume. The decay length for conventional SPR is significantly larger (200−300 nm)[18] than that of LSPR (∼20−30 nm).[19,20] Because of this big difference in decay length and thus sensing volume, it is important to distinguish between bulk refractive index sensitivity (η_B) and surface refractive index sensitivity (η_S). Despite a significantly larger bulk refractive index sensitivity for conventional SPR compared to LSPR, the two sensing schemes show comparable biosensing performances.[21,22]

Received: August 15, 2013
Revised: October 10, 2013
Published: October 10, 2013

For conventional SPR, the sensitivity is primarily dependent on resonance wavelength or incidence angle, while for LSPR-based sensors it mainly relies on the nature of the metal nanostructures. A variety of nanostructures have been evaluated as transducers for refractive index sensing such as gold nanorods,[11,23,24] gold nanoshells,[25] silver nanocubes,[26] gold nanobipyramids,[11,27] gold nanostars,[28] and silver nanoprisms.[29−31] Anisotropic nanostructures with sharp features exhibit particularly high refractive index sensitivities[27] due to increased electromagnetic fields at the sharp corners. Unfortunately, silver nanoparticles and sharp-tipped silver nanostructures in particular suffer from morphological instability leading to truncation or rounding of the tips and corners, which drastically reduces their sensitivity in detecting small refractive index changes. This is particularly problematic in presence of buffers with high ionic strengths, where silver nanoprisms are rapidly oxidized and etched.[32] This can however be prevented by addition of a thin gold layer to unstable (110) facets of silver nanoprisms (SNPs) on their edges which protects them from being etched. These gold-coated nanostructures take advantage of the high sensitivity of SNPs and the stability and functionalizability of gold,[33] making them attractive transducer elements for optical biosensing that remain intact and stable even at physiological ionic strength. Other approaches has been reported to stabilize SNPs such as silica coating and oligonucleotide conjugation,[34−36] but since the coating often is rather thick this will result in loss in sensitivity. Moreover, these stabilization strategies do not provide as convenient and flexible possibilities for further surface functionalization as a bare gold surface amenable to gold−thiol chemistry. Gold coating of silver nanostructures is thus a very effective and facile approach for realizing stable and highly sensitive LSPR-based sensors.

In this study we have investigated bulk refractive index sensitivity and surface refractive index sensitivity for edge gold-coated silver nanoprisms (GSNPs) and compared them to both conventional SPR using a flat gold film and gold nanospheres. Sucrose−water mixtures were used to determine the bulk refractive index sensitivity, while adsorption of oppositely charged polyelectrolytes and a model protein was used to study the local refractive index changes in order to determine surface sensitivity and sensing volume. By exploring the surface sensitivity of various nanostructures, it is possible to design a biosensing system based on LSPR with an optimal sensing volume. Molecular binding events typically take place close to the sensor surface and the ability to detect local changes close to the surface is thus of great importance in order to maximize the sensitivity and optimize the sensing performance.

EXPERIMENTAL DETAILS

Silver Colloid Synthesis. Ag colloids were prepared using a previously reported protocol.[37]

Photomediated Silver Nanoprism Growth. In a typical experiment, 25 mL of the spherical silver colloid solution prepared in the previous step was irradiated with a 150 W halogen lamp coupled with an optical bandpass filter centered at 500 ± 20 nm. The photoreaction was monitored by UV−vis spectroscopy. The silver colloid exhibited purple color with one major extinction band at around 600 ± 50 nm, indicating the formation of silver nanoprisms. In order to make nanoprisms with larger edge lengths, the purple solution was irradiated with 600 ± 20 nm bandpass filter. The silver solution at the end of this step has green color with a major SPR band at around 700 ± 50 nm. These solutions were then centrifuged, and the Ag nanoprisms were redispersed into a pure solution of trisodium citrate (0.3 mM); this helps to remove the bis(*p*-sulfonatophenyl)phenylphosphine) in the Ag nanoprism solution.

Synthesis of Edge-Gold Coated Silver Nanoprisms (GSNPs). GSNPs were prepared by using a modification of previously reported protocol.[38] Typically to 25 mL of Millipore water in a glass vial kept in an ice bath, 15 mL of Ag nanoprism solution was added and the resulting solution stirred for 30 min. This was followed by infusion of 3 mM basic NH_2OH·HCl and 0.37 mM $HAuCl_4$ by two separate tubes using a programmable syringe pump. The solution was vigorously stirred during the injection process (1 mL/hour) for up to 40 min. The injection time depends on the gold frame ridge thickness which is desirable. The basic NH_2OH·HCl solution is prepared by adding 300 μL of NaOH (0.5 M) to 10 mL as prepared NH_2OH·HCl.

Spherical Gold Nanoparticles. Spherical gold colloids with a diameter of 50 nm were purchased from British BioCell International.

Transmission Electron Microscopy. Samples were prepared for electron microscopy by depositing and drying of a drop of an aqueous particle solution on top of a carbon-coated 300 mesh copper grid (Ted Pella, Inc.). For TEM measurements, the solution is washed with pure ethanol, and after that a concentrated solution is dropped on a lacey carbon TEM support 300 mesh copper grid and dried at room temperature. TEM measurements were carried out with either JEOL JEM-2100 LaB6 or JEM-2100 both operating at 200 kV. The HAADF-STEM imaging was carried out with a FEI Titan TEM with a Schottky electron source, operated at 200 kV. TEM images were taken close to Scherzer defocus. The STEM images were obtained using an electron probe with an approximate diameter of 0.2 nm.

Conventional SPR Experiments. Glass surfaces (12 × 12 mm^2) coated with a 45 nm thin gold film (GE Healthcare) were used for the SPR measurements. Prior to use, all SPR surfaces were cleaned in a solution containing a 5:1:1 mixture by volume with Milli-Q water (Milli-Q, Millipore), 30% hydrogen peroxide (Merck KGaA), and 25% ammonia (Merck KGaA) for at least 10 min at 85 °C followed by thorough rinsing with Milli-Q water.

Measurements were carried out on a custom-built instrument, described in more detail elsewhere.[39] Briefly, the SPR setup was based on the Kretschmann configuration and had two motorized angular rotation stages (RV160, Newport Inc.) with a CCD detector (Retiga Exi, Qimaging Corp., 12 bit 1 MP) mounted on one of the arms. Light from a monochromator (SpectraPro 300i, Acton Research Corp.) was collimated and TM-polarized and finally guided to the prism (BK7 glass, Melles Griot), where the SPR sensor surface was placed. Measurements were performed with a fixed angle of incident of 72° and a wavelength interval of 500−900 nm with a sampling rate of 100 nm/min. Solutions were introduced to the sensor surface using an open incubation cell with a volume of 1 mL, sealed to the surface using a nitrile rubber O-ring. The wavelength dependence of the monochromator efficiency was normalized using TE-polarized light, which was divided with the reflectivity spectra obtained from TM-polarized light. The instrument was controlled, and SPR data were collected and analyzed using a software program written in LabView (National Instruments Corp.).

dx.doi.org/10.1021/jp408187e | J. Phys. Chem. C 2013, 117, 23148−23154

LSPR Experiments. Both bulk and surface sensitivity measurements were conducted using a Tecan Sapphire II plate reader. Gold nanoparticles were electrostatically immobilized in pretreated polystyrene microwell plates (Nalge Nunc International) using oppositely charged polyelectrolytes. Polyelectrolyte solutions of polyethylenimine (PEI, M_w 750 000, Sigma-Aldrich), polystyrenesulfonate (PSS, M_w 75 000, Sigma-Aldrich), and poly(allylamine hydrochloride) (PAH, M_w 56 000, Sigma-Aldrich) were prepared with a concentration of 2 mg/mL in 0.5 M NaCl (Sigma-Aldrich) aqueous solutions. The wells were incubated with 150 μL of polyelectrolyte solutions for 15 min in the order PEI/PSS/PAH with a thorough rinsing of Milli-Q water between each deposition. This creates a layer-by-layer structure with positively charged PAH as the top layer which enables an electrostatic immobilization of negatively charged citrate-stabilized nanoparticles. Concentrated nanoparticle solutions (150 μL) were deposited in the pretreated wells and left for incubation overnight. The wells were rinsed with Milli-Q water before bulk sensitivity measurements with sucrose or surface sensitivity measurements with polyelectrolytes or protein were conducted.

Bulk Refractive Index Sensitivity Measurement. Water−sucrose mixtures were used in order to determine the bulk refractive index sensitivity for both types of metal nanoparticles and conventional SPR. The concentration of sucrose (Merck KGaA) in the aqueous mixtures was varied from 0% (w/w) to 50% in steps of 10% ranging from n = 1.333 to 1.420 in refractive index. The sensitivity was determined by plotting the wavelength where SPR reflectivity minimum (λ_{SPR}) or LSPR peak maximum (λ_{LSPR}) occurs, both as a function of the refractive index.

Local Refractive Index Sensitivity Measurement. A layer-by-layer assembly of polyelectrolytes was used to evaluate the surface refractive index sensitivity. Five bilayers of PAH/PSS (2 mg/mL in 0.5 M NaCl aqueous solutions) were built up by incubating a continuous gold or nanoparticle coated surface in PAH and PSS for 15 min, respectively, with a thorough rinsing of Milli-Q water between each deposition. The thickness of the PAH/PSS layers was evaluated in dry state by null ellipsometry using a Rudolph Research AutoEl III ellipsometer equipped with a He−Ne laser (λ = 632.8 nm) with an angle of incidence of 70°. A one-film model assuming a thin, transparent organic layer with a refractive index of n = 1.5 was used to determine the thickness of the PE layers. The surface refractive index sensitivity was also examined by adsorption of BSA (Sigma-Aldrich, 1 mg/mL in PBS, pH 7.0 for 30 min).

RESULTS AND DISCUSSION

Silver nanoprisms were synthesized using a photomediated growth method and coated with a thin layer of gold by carefully reducing gold salt using hydroxylamine (HyA). A thorough investigation of the synthesis of these nanostructures has been reported previously by Shahjamali et al.[37] The plasmon frequency of the GSNPs is highly tunable by varying the size and shape of either the silver core or the surrounding gold layer. The bare SNPs used in this study have an edge length of about 30−40 nm with a plasmon peak position at ∼600 nm and a gold frame thickness of about 2−4 nm (Figure 1) which redshifts the plasmon peak 30−70 nm depending on the thickness of the added gold frame (Figure S1, Supporting Information). Larger nanoprisms and thicker gold frames result in larger redshifts of the plasmon peak which actually gives rise to an increased sensitivity but also increases multipolar excitation and

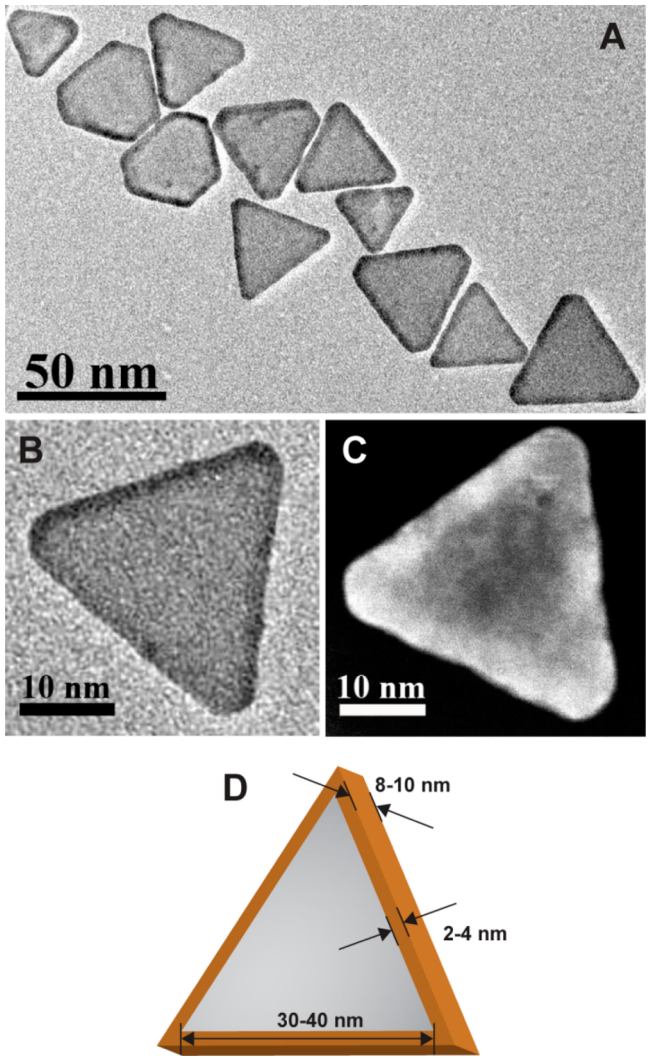

Figure 1. (A, B) Bright-field TEM image of edge gold-coated nanoprisms (GSNPs). (C) STEM-HAADF image of a GSNP clearly shows the gold deposition on the edges (brighter portion) of an Ag nanoprism. (D) An illustration showing the general dimensions of a GSNP.

radiative damping resulting in a broadening of the plasmon peak and a reduction of the resolution.[31] Otte et al. have shown both theoretically and experimentally that the optimum LSPR sensing region corresponds to nanostructures with an excitation resonance around 700 nm.[40] With this in mind we synthesized particles with a plasmon peak position in this region. The position also coincides well with the plasmon resonance position of conventional SPR, enabling a fair comparison between the two systems. Figure of merit (FOM) is commonly used to quantify the relationship between sensitivity and resolution and is defined as FOM = η/fwhm, where fwhm is the full width at half-maximum of the LSPR peak.

Bulk Refractive Index Sensing. Bulk sensitivity measurements were performed by varying the refractive index of the surrounding medium using aqueous solutions of sucrose at different concentrations (0−50% sucrose). Figure 2 summarizes the bulk RI sensitivity for the GSNPs, conventional SPR (flat gold film), and 50 nm gold nanospheres. As expected, the response obtained from propagating surface plasmons increased exponentially and a nonlinear relationship over the entire wavelength region was observed. Conventional SPR biosensing

dx.doi.org/10.1021/jp408187e | J. Phys. Chem. C 2013, 117, 23148−23154

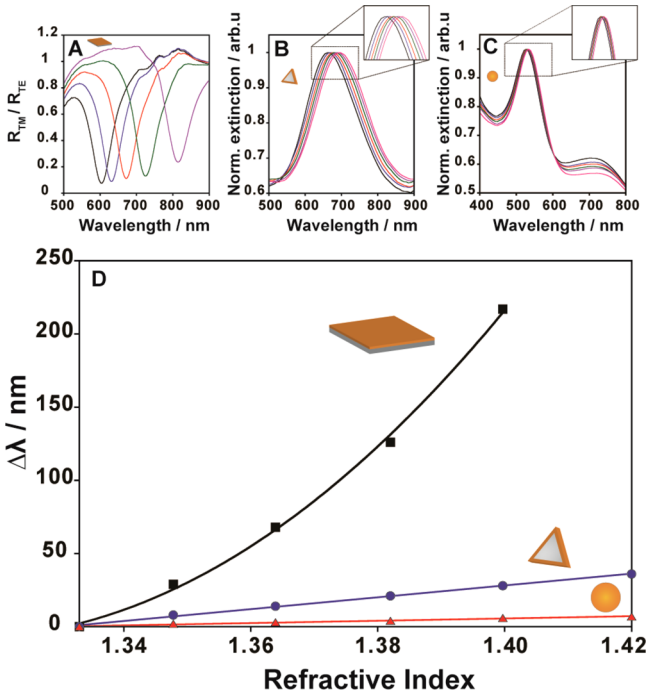

Figure 2. Bulk refractive index sensitivity spectra for conventional SPR (flat gold film) (A), GSNPs (B), and gold nanospheres (C) obtained from solutions with increasing sucrose concentrations 0–50%. (D) Spectral shifts ($\Delta\lambda_{SPR}$ and $\Delta\lambda_{LSPR}$) as a function of refractive index.

setups are typically used to detect quite small changes in the refractive index (n_{water} = 1.33 and $n_{biomolecule}$ = 1.46), and measurements are hence performed in a narrow wavelength region where nonlinearities usually are not problematic. The bulk RI sensitivity (η_B) for the conventional SPR setup used in this study varied from 1500 nm/RIU to 3500 nm/RIU depending on the wavelength region. At 650 nm, where the LSPR peak of the GSNPs has its maximum, the bulk sensitivity was 2500 nm/RIU for the conventional SPR. The response caused by the 50% sucrose–water mixture could not be obtained because the shift exceeded the detection range of the instrument. For the two different nanoparticle structures, the position of the plasmon resonance peak red-shifted linearly with increasing refractive index of the surrounding media. The bulk RI sensitivity of the GSNPs was determined by linear regression to be $\eta_B \sim 425$ nm/RIU with a FOM of ~3 (fwhm ~ 145 nm). Higher sensitivities were obtained in other batches of GSNPs with slightly different sizes and thickness of the gold coating (Figure S2, Supporting Information) but with lower FOM values. Other reports on pure silver nanoprisms with a similar LSPR peak position show a slightly lower bulk RI sensitivity compared to the value obtained here for GSNPs.[31] The higher sensitivity obtained here is probably due to a lower degree of truncation of the GSNPs because of the gold frame which protects the sharp tips of the prisms. η_B for the spherical gold nanoparticles (d = 50 nm) was determined to be ~85 nm/RIU, a value that corresponds well with previously reported results.[11] Conventional SPR thus exhibits roughly 1 order of magnitude higher bulk RI sensitivity compared to the nanoparticles used in this study.

Bulk RI measurements were performed on nanoparticles immobilized on plastic substrates covered with polyelectrolyte layers (PEL). Nanoparticles bound to substrates typically display a lower bulk refractive index sensitivity compared to dispersed particles since attached particles experience an inhomogeneous dielectric environment. This is especially true for nanoparticles with a flat structure like nanoprisms. However, in comparative experiments with dispersed and immobilized nanoparticles very similar bulk RI sensitivity was obtained (Figure S3, Supporting Information). A likely explanation is that nanoparticles electrostatically adsorbed to PEL are not as rigidly attached as nanoparticles immobilized on silanized glass substrates. Also, the swelling of the polyelectrolytes enables the water–sucrose solution to access the bottom surface as well, thus creating a fairly homogeneous surrounding.

Local Refractive Index Sensing. The refractive index sensitivity in SPR and LSPR is strongly related to both intensity and decay length of the local electromagnetic (EM) field created at the resonance plasmon frequency. The decay length of the EM-field depends on several parameters including structure, geometry, material, surrounding environment, etc.,[7,41,42] which means that the local refractive index sensitivity and sensing volume can differentiate quite a lot between various nanoparticles. Surface sensitivity (η_S) is a measure of the response induced by a local change in the refractive index in close proximity to the sensing element while the sensing volume is a measure of how far from the sensing surface these changes can be detected. Both surface RI sensitivity and sensing volume can be determined by adsorbing polyelectrolyte multilayers which is a commonly used technique to form thin films at surfaces with thickness control at the nanometer scale.[43,44] Two frequently used polyelectrolytes, polystyrenesulfonate (PSS) and poly(allylamine hydrochloride) (PAH), were used in this study to monitor the response from the plasmonic structures and determine their surface sensitivity.

The thickness of a bilayer of PAH/PSS was determined by null ellipsometry to be 3 ± 0.2 nm (Figure 3D inset). This value was however determined in air while the surface sensitivity measurements were conducted in aqueous media. A swelling of about 30% of the PEL is expected in water.[45] This also creates a less dense polymer matrix which reduces the refractive index of the polymer film thus, generating a smaller change in the refractive index detection.

Spectra were collected after each polyelectrolyte bilayer deposition (Figure 3A–C), and the position of the SPR dip and the LSPR peak maximum for the two nanoparticles were plotted as a function of the number of PELs (Figure 3D). GSNPs showed a substantial red-shift of about ~45 nm for the first bilayer of PAH/PSS. The extent of the red-shift was then reduced for every additional PEL added, to ~7 nm/bilayer for a change from 8 to 10 PELs. A continuation of added PELs beyond 10 layers would most probably result in an additional reduction of the observed red-shift. The response acquired from conventional SPR resulted in a more linear response with increasing number of PELs. In contrast to the nanoparticles, an increase in the shift with increasing film thickness was observed with conventional SPR, which can be explained by the wavelength dependence of the plasmon resonance as seen in the bulk sensitivity experiments (Figure 2). Spherical nanoparticles showed a similar trend as the nanoprisms, but the response was almost one order of magnitude lower. The results from the surface sensitivity measurements using polyelectrolyte multilayers showed that the GSNPs exhibit a high sensitivity for detection of small, local refractive index changes closer than 10 nm from the sensing surface and are about 4 times more sensitive than conventional SPR.

dx.doi.org/10.1021/jp408187e | J. Phys. Chem. C 2013, 117, 23148–23154

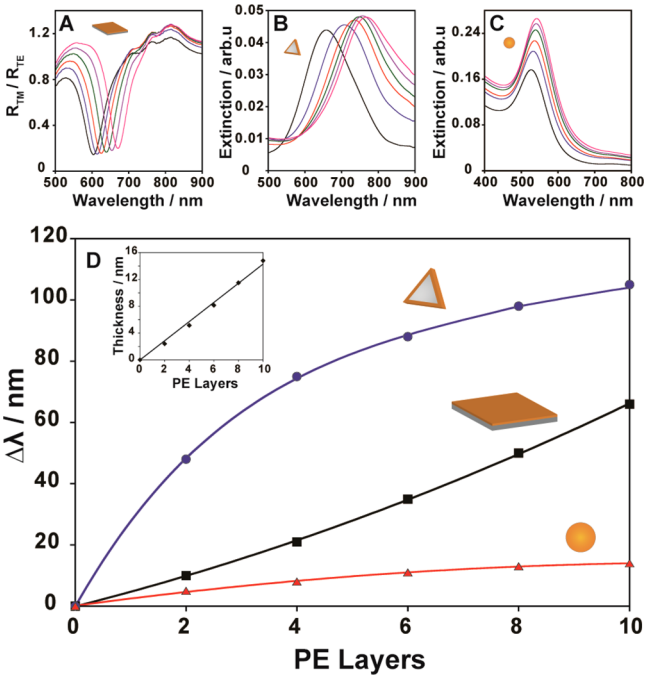

Figure 3. Reflection spectra for conventional SPR (flat gold film) (A) and extinction spectra for GSNPs (B) and gold nanospheres (C) upon increasing number of polyelectrolyte layers (0 to 10). (D) Surface refractive index sensitivity obtained by plotting the spectral shift seen in (A–C) as a function of increasing polyelectrolyte layers. The inset shows how the thickness increases linearly with increasing number of PAH/PSS layers, determined by null ellipsometry in the dried state.

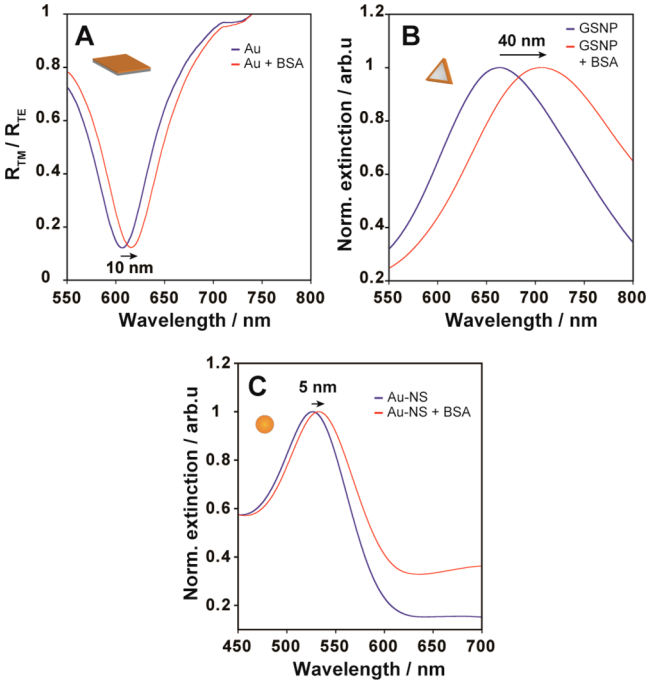

Figure 4. Spectral shifts ($\Delta\lambda_{SPR}$ and $\Delta\lambda_{LSPR}$) obtained upon absorption of BSA (1 mg/mL) for SPR (A), GSNPs (B), and gold nanospheres (C).

In order to verify that the shift in the LSPR peak position of the GSNPs was not caused by oxidation and etching of the silver core, the particles were exposed to hydrogen peroxide. Etching of the silver core using hydrogen peroxide resulted in a drastic reduction in the intensity of the LSPR peak but only a minor red-shift was observed (Figure S4, Supporting Information). No reduction in the LSPR peak intensity was seen in the experiments with the polyelectrolytes, which confirms that the large red-shifts observed in these experiments were caused by the high local refractive index sensitivity of the particles.

The surface refractive index sensitivity was also examined by physisorption of bovine serum albumin (BSA) onto the plasmonic substrates to confirm the results obtained with PELs. Figure 4 shows UV–vis spectra observed before and after incubation with BSA (1 mg/mL) for the three different systems. One adsorbed layer of BSA resulted in a 40 nm red-shift of the LSPR peak position for GSNPs, compared to a shift of 10 nm for conventional SPR and 5 nm for spherical gold nanoparticles. Based on the shifts obtained when adsorbing a bilayer of PAH/PSS, these results indicate the presence of a protein film of about 3 nm, which corresponds well with the reported thickness of an adsorbed monolayer of BSA.[46]

The GSNPs examined in this work exhibit a highly local sensitivity with a sensing volume of about ~15 nm. This means that the molecular sensing event needs to be kept close to the particles in order to observe the interaction of interest which reduces the possibility to use polymer matrixes or sandwich assays and also excludes the study of larger molecular systems. Sensing elements with a highly local sensing volume are more suitable for detecting small molecules which only induces a small change in the surrounding dielectric environment. Molecules with low molecular masses are problematic to detect using a conventional SPR setup since their contribution to the signal tends to be masked by the high bulk response created because of the large sensing volume. As this large bulk response is not observed with LSPR-based sensing systems, the nanostructures presented here allow for the development of robust and low-cost bioanalytical devices that are more sensitive in detecting small target molecules than conventional planar SPR-based biosensors. Future work will focus on functionalization and optimization of the nanostructures to further increase their potential for LSPR-based biosensing.

CONCLUSIONS

We have presented an experimental comparison between bulk and surface refractive index sensitivity for propagating surface plasmons on a planar, thin gold film and localized surface plasmons in edge gold-coated silver nanoprisms and gold nanospheres. Conventional SPR based on propagating surface plasmons exhibit 1 order of magnitude higher bulk refractive index sensitivity compared to LSPR-based nanosensors. However, LSPR-based systems exhibit similar or even higher sensitivity close to the surface due to the shorter decay length of the electromagnetic field. We have demonstrated that silver nanoprisms covered with a protecting gold frame are associated with a 4-fold higher sensitivity compared to conventional SPR and an 8-fold higher sensitivity compared to spherical gold nanoparticles with respect to detecting refractive index changes in close proximity (<10 nm) to the sensing surface. This is particularly interesting in the context of small molecule detection.

ASSOCIATED CONTENT

Supporting Information

LSPR peak evolution during edge gold-coating, UV–vis spectra and bulk RI sensitivities for six different batches of GSNPs,

dx.doi.org/10.1021/jp408187e | J. Phys. Chem. C 2013, 117, 23148–23154

comparison of bulk refractive index sensitivity for GSNPs and gold nanospheres immobilized on a substrate and in solution, and the effect on UV−vis spectra upon oxidation of GSNPs using hydrogen peroxide. This material is available free of charge via the Internet at http://pubs.acs.org.

AUTHOR INFORMATION

Corresponding Author

*E-mail daniel.aili@liu.se (D.A.).

Notes

The authors declare no competing financial interest.

ACKNOWLEDGMENTS

We acknowledge Prof. Borja Sepulveda for helpful discussions. The authors are grateful for financial support from the Swedish Research Council (VR), the Swedish Foundation for Strategic Research (SSF), the Knut and Alice Wallenberg Foundation (KAW), and the Centre in Nano science and technology (CeNano). During this study E.M. was enrolled in the graduate school Forum Scientium. M.M.S. and C.X. thank the support from Singapore MOE AcRF-Tier1 (RG 44/11) and AcRF-Tier2 (MOE2012-T2-2-041, ARC 5/13), and CRP program (NRF-CRP5-2009-04) from NRF Singapore. This research is also supported by Science & Engineering Research Council (SERC) of Agency for Science, Technology and Research (A*STAR), for the TSRP project under the number of 102 152 0015.

ABBREVIATIONS

LSPR, localized surface plasmon resonance; GSNP, edge gold-coated silver nanoprisms; SPR, surface plasmon resonance; SNP, silver nanoprism; RI, refractive index; HyA, hydroxylamine; FOM, figure of merit; PEL, polyelectrolyte layers; EM, electromagnetic; PSS, polystyrenesulfonate; PAH, poly(allylamine hydrochloride); BSA, bovine serum albumin.

REFERENCES

(1) Liedberg, B.; Nylander, C.; Lundstrom, I. Surface-Plasmon Resonance for Gas-Detection and Biosensing. *Sens. Actuators* **1983**, *4*, 299−304.

(2) Knoll, W. Interfaces and Thin Films as Seen by Bound Electromagnetic Waves. *Annu. Rev. Phys. Chem.* **1998**, *49*, 569−638.

(3) Homola, J.; Koudela, I.; Yee, S. S. Surface Plasmon Resonance Sensors Based on Diffraction Gratings and Prism Couplers: Sensitivity Comparison. *Sens. Actuators, B* **1999**, *54*, 16−24.

(4) Homola, J. Surface Plasmon Resonance Sensors for Detection of Chemical and Biological Species. *Chem. Rev.* **2008**, *108*, 462−493.

(5) Situ, C.; Buijs, J.; Mooney, M. H.; Elliott, C. T. Advances in Surface Plasmon Resonance Biosensor Technology Towards High-Throughput, Food-Safety Analysis. *TrAC, Trends Anal. Chem.* **2010**, *29*, 1305−1315.

(6) Shankaran, D. R.; Gobi, K. V. A.; Miura, N. Recent Advancements in Surface Plasmon Resonance Immunosensors for Detection of Small Molecules of Biomedical, Food and Environmental Interest. *Sens. Actuators, B* **2007**, *121*, 158−177.

(7) Haes, A. J.; Van Duyne, R. P. A Unified View of Propagating and Localized Surface Plasmon Resonance Biosensors. *Anal. Bioanal. Chem.* **2004**, *379*, 920−930.

(8) Willets, K. A.; Van Duyne, R. P. Localized Surface Plasmon Resonance Spectroscopy and Sensing. *Annu. Rev. Phys. Chem.* **2007**, *58*, 267−297.

(9) Anker, J. N.; Hall, W. P.; Lyandres, O.; Shah, N. C.; Zhao, J.; Van Duyne, R. P. Biosensing with Plasmonic Nanosensors. *Nat. Mater.* **2008**, *7*, 442−453.

(10) Hutter, E.; Fendler, J. H. Exploitation of Localized Surface Plasmon Resonance. *Adv. Mater.* **2004**, *16*, 1685−1706.

(11) Chen, H. J.; Kou, X. S.; Yang, Z.; Ni, W. H.; Wang, J. F. Shape- and Size-Dependent Refractive Index Sensitivity of Gold Nanoparticles. *Langmuir* **2008**, *24*, 5233−5237.

(12) Noguez, C. Surface Plasmons on Metal Nanoparticles: The Influence of Shape and Physical Environment. *J. Phys. Chem. C* **2007**, *111*, 3806−3819.

(13) Kelly, K. L.; Coronado, E.; Zhao, L. L.; Schatz, G. C. The Optical Properties of Metal Nanoparticles: The Influence of Size, Shape, and Dielectric Environment. *J. Phys. Chem. B* **2003**, *107*, 668−677.

(14) Novak, J. P.; Feldheim, D. L. Assembly of Phenylacetylene-Bridged Silver and Gold Nanoparticle Arrays. *J. Am. Chem. Soc.* **2000**, *122*, 3979−3980.

(15) Elghanian, R.; Storhoff, J. J.; Mucic, R. C.; Letsinger, R. L.; Mirkin, C. A. Selective Colorimetric Detection of Polynucleotides Based on the Distance-Dependent Optical Properties of Gold Nanoparticles. *Science* **1997**, *277*, 1078−1081.

(16) Aili, D.; Gryko, P.; Sepulveda, B.; Dick, J. A. G.; Kirby, N.; Heenan, R.; Baltzer, L.; Liedberg, B.; Ryan, M. P.; Stevens, M. M. Polypeptide Folding-Mediated Tuning of the Optical and Structural Properties of Gold Nanoparticle Assemblies. *Nano Lett.* **2011**, *11*, 5564−5573.

(17) Sepulveda, B.; Angelome, P. C.; Lechuga, L. M.; Liz-Marzan, L. M. LSPR-Based Nanobiosensors. *Nano Today* **2009**, *4*, 244−251.

(18) Jung, L. S.; Campbell, C. T.; Chinowsky, T. M.; Mar, M. N.; Yee, S. S. Quantitative Interpretation of the Response of Surface Plasmon Resonance Sensors to Adsorbed Films. *Langmuir* **1998**, *14*, 5636−5648.

(19) Malinsky, M. D.; Kelly, K. L.; Schatz, G. C.; Van Duyne, R. P. Chain Length Dependence and Sensing Capabilities of the Localized Surface Plasmon Resonance of Silver Nanoparticles Chemically Modified with Alkanethiol Self-Assembled Monolayers. *J. Am. Chem. Soc.* **2001**, *123*, 1471−1482.

(20) Live, L. S.; Masson, J. F. High Sensitivity of Plasmonic Microstructures Near the Transition From Short-Range to Propagating Surface Plasmon. *J. Phys. Chem. C* **2009**, *113*, 10052−10060.

(21) Yonzon, C. R.; Jeoungf, E.; Zou, S. L.; Schatz, G. C.; Mrksich, M.; Van Duyne, R. P. A Comparative Analysis of Localized and Propagating Surface Plasmon Resonance Sensors: The Binding of Concanavalin A to a Monosaccharide Functionalized Self-Assembled Monolayer. *J. Am. Chem. Soc.* **2004**, *126*, 12669−12676.

(22) Svedendahl, M.; Chen, S.; Dmitriev, A.; Kall, M. Refractometric Sensing Using Propagating Versus Localized Surface Plasmons: A Direct Comparison. *Nano Lett.* **2009**, *9*, 4428−4433.

(23) Nusz, G. J.; Curry, A. C.; Marinakos, S. M.; Wax, A.; Chilkoti, A. Rational Selection of Gold Nanorod Geometry for Label-Free Plasmonic Biosensors. *ACS Nano* **2009**, *3*, 795−806.

(24) Mayer, K. M.; Lee, S.; Liao, H.; Rostro, B. C.; Fuentes, A.; Scully, P. T.; Nehl, C. L.; Hafner, J. H. A Label-Free Immunoassay Based Upon Localized Surface Plasmon Resonance of Gold Nanorods. *ACS Nano* **2008**, *2*, 687−692.

(25) Sun, Y. G.; Xia, Y. N. Increased Sensitivity of Surface Plasmon Resonance of Gold Nanoshells Compared to That of Gold Solid Colloids in Response to Environmental Changes. *Anal. Chem.* **2002**, *74*, 5297−5305.

(26) Sherry, L. J.; Chang, S. H.; Schatz, G. C.; Van Duyne, R. P.; Wiley, B. J.; Xia, Y. N. Localized Surface Plasmon Resonance Spectroscopy of Single Silver Nanocubes. *Nano Lett.* **2005**, *5*, 2034−2038.

(27) Burgin, J.; Liu, M. Z.; Guyot-Sionnest, P. Dielectric Sensing with Deposited Gold Bipyramids. *J. Phys. Chem. C* **2008**, *112*, 19279−19282.

(28) Nehl, C. L.; Liao, H. W.; Hafner, J. H. Optical Properties of Star-Shaped Gold Nanoparticles. *Nano Lett.* **2006**, *6*, 683−688.

(29) Mcfarland, A. D.; Van Duyne, R. P. Single Silver Nanoparticles as Real-Time Optical Sensors with Zeptomole Sensitivity. *Nano Lett.* **2003**, *3*, 1057−1062.

(30) Sherry, L. J.; Jin, R. C.; Mirkin, C. A.; Schatz, G. C.; Van Duyne, R. P. Localized Surface Plasmon Resonance Spectroscopy of Single Silver Triangular Nanoprisms. *Nano Lett.* **2006**, *6*, 2060−2065.
(31) Charles, D. E.; Aherne, D.; Gara, M.; Ledwith, D. M.; Gun'ko, Y. K.; Kelly, J. M.; Blau, W. J.; Brennan-Fournet, M. E. Versatile Solution Phase Triangular Silver Nanoplates for Highly Sensitive Plasmon Resonance Sensing. *ACS Nano* **2010**, *4*, 55−64.
(32) Jiang, X. C.; Yu, A. B. Silver Nanoplates: A Highly Sensitive Material Toward Inorganic Anions. *Langmuir* **2008**, *24*, 4300−4309.
(33) Han, G.; Ghosh, P.; Rotello, V. M. Functionalized Gold Nanoparticles for Drug Delivery. *Nanomedicine* **2007**, *2*, 113−123.
(34) Banholzer, M. J.; Harris, N.; Millstone, J. E.; Schatz, G. C.; Mirkin, C. A. Abnormally Large Plasmonic Shifts in Silica-Protected Gold Triangular Nanoprisms. *J. Phys. Chem. C* **2010**, *114*, 7521−7526.
(35) Xue, C.; Chen, X.; Hurst, S. J.; Mirkin, C. A. Self-Assembled Monolayer Mediated Silica Coating of Silver Triangular Nanoprisms. *Adv. Mater.* **2007**, *19*, 4071−4074.
(36) Lee, J. S.; Lytton-Jean, A. K. R.; Hurst, S. J.; Mirkin, C. A. Silver Nanoparticle-Oligonucleotide Conjugates Based on DNA with Triple Cyclic Disulfide Moieties. *Nano Lett.* **2007**, *7*, 2112−2115.
(37) Shahjamali, M. M.; Bosman, M.; Cao, S. W.; Huang, X.; Saadat, S.; Martinsson, E.; Aili, D.; Tay, Y. Y.; Liedberg, B.; Loo, S. C. J.; Zhang, H.; Boey, F.; Xue, C. Gold Coating of Silver Nanoprisms. *Adv. Funct. Mater.* **2012**, *22*, 849−854.
(38) Shahjamali, M. M.; Bosman, M.; Cao, S.; Huang, X.; Cao, X.; Zhang, H.; Pramana, S. S.; Xue, C. Surfactant-Free Sub-2 Nm Ultrathin Triangular Gold Nanoframes. *Small* **2013**, *9*, 2880−2886.
(39) Andersson, O.; Larsson, A.; Ekblad, T.; Liedberg, B. Gradient Hydrogel Matrix for Microarray and Biosensor Applications: An Imaging SPR Study. *Biomacromolecules* **2009**, *10*, 142−148.
(40) Otte, M. A.; Sepulveda, B.; Ni, W. H.; Juste, J. P.; Liz-Marzan, L. M.; Lechuga, L. M. Identification of the Optimal Spectral Region for Plasmonic and Nanoplasmonic Sensing. *ACS Nano* **2010**, *4*, 349−357.
(41) Bukasov, R.; Ali, T. A.; Nordlander, P.; Shumaker-Parry, J. S. Probing the Plasmonic Near-Field of Gold Nanocrescent Antennas. *ACS Nano* **2010**, *4*, 6639−6650.
(42) Haes, A. J.; Zou, S. L.; Schatz, G. C.; Van Duyne, R. P. A Nanoscale Optical Biosensor: The Long Range Distance Dependence of the Localized Surface Plasmon Resonance of Noble Metal Nanoparticles. *J. Phys. Chem. B* **2004**, *108*, 109−116.
(43) Decher, G.; Hong, J. D.; Schmitt, J. Buildup of Ultrathin Multilayer Films by a Self-Assembly Process. III Consecutively Alternating Adsorption of Anionic and Cationic Polyelectrolytes on Charged Surfaces. *Thin Solid Films* **1992**, *210*, 831−835.
(44) Bertrand, P.; Jonas, A.; Laschewsky, A.; Legras, R. Ultrathin Polymer Coatings by Complexation of Polyelectrolytes at Interfaces: Suitable Materials, Structure and Properties. *Macromol. Rapid Commun.* **2000**, *21*, 319−348.
(45) Wong, J. E.; Rehfeldt, F.; Hanni, P.; Tanaka, M.; Klitzing, R. V. Swelling Behavior of Polyelectrolyte Multilayers in Saturated Water Vapor. *Macromolecules* **2004**, *37*, 7285−7289.
(46) Mcclellan, S. J.; Franses, E. I. Adsorption of Bovine Serum Albumin at Solid/Aqueous Interfaces. *Colloids Surf., A* **2005**, *260*, 265−275.